Design of a parallel crank-rocker flapping mechanism for insect-inspired micro air vehicles

A T Conn, S C Burgess*, and **C S Ling**
Department of Mechanical Engineering, University of Bristol, Bristol, UK

The manuscript was received on 10 October 2006 and was accepted after revision for publication on 18 April 2007.

DOI: 10.1243/09544062JMES517

Abstract: In the current paper, a novel micro air vehicle (MAV) flapping mechanism for replicating insect wing kinematics is presented. Insects flap their wings in a complex motion that enables them to generate several unsteady aerodynamic mechanisms, which are extremely beneficial for lift production. A flapping wing MAV that can reproduce these aerodynamic mechanisms in a controlled manner is likely to outperform alternative flight platforms such as rotary wing MAVs. A biomimetic design approach was undertaken to develop a novel flapping mechanism, the parallel crank-rocker (PCR). Unlike several existing flapping mechanisms (which are compared using an original classification method), the PCR mechanism has an integrated flapping and pitching output motion which is not constrained. This allows the wing angle of attack, a key kinematic parameter, to be adjusted and enables the MAV to enact manoeuvres and have flight stability. Testing of a near-MAV scale PCR prototype using a high-speed camera showed that the flapping angle and adjustable angle of attack both closely matched predicted values, proving the mechanism can replicate insect wing kinematics. A mean lift force of 3.35 g was measured with the prototype in a hovering orientation and flapping at 7.15 Hz.

Keywords: insect flight, flapping wings, micro air vehicle, biomimetics, bio-inspired design

1 INTRODUCTION

A micro air vehicle (MAV) is an autonomous miniature flying craft capable of performing a variety of novel military and civil applications. It is a unique class of air vehicle that in terms of size and mass is at least an order of magnitude smaller than the current military unmanned air vehicles. The desire to develop MAVs was founded on the increasing miniaturization of electro-mechanical technologies over the last few decades that created opportunities for a variety of novel military and civil applications. In particular, the US Defense Advanced Research Projects Agency (DARPA) became interested in the reconnaissance, surveillance, and substance detection capabilities afforded by miniature digital cameras and microelectromechanical systems [**1**]. DARPA's involvement in the initiation of MAV research is notable for the 15 cm dimensional limit they set, which is now the most commonly quoted definition of a MAV.

Although all MAVs are defined by the 15 cm dimensional limit, there is no restriction on the selection of flight platform and propulsion technology. However, certain flight platforms are inherently biased to particular types of operation. Of the three most viable platforms (fixed wing, rotary wing, and flapping wing) it is generally accepted that fixed wing MAVs are better optimized towards outdoor missions with higher endurance, while the other two have the benefit of being able to hover and manoeuvre through confined indoor environments. Although rotary wings are a far more proven and established flight platform, research into the flight of insects and small hummingbirds suggests a flapping wing MAV may be preferable.

It has been found that these natural flyers achieve their considerable flight performance through the exploitation of the low Reynolds number

**Corresponding author: Department of Mechanical Engineering, University of Bristol, Queen's Building, University Walk, Bristol BS8 1TR, UK. email: s.c.burgess@bris.ac.uk*

flow regime they share with MAVs. Researchers proved that by employing a range of unsteady aerodynamic phenomena in addition to the aerofoil effect they could generate substantial lift and thrust forces [**2**]. This has led to these unsteady aerodynamic phenomena being considered for implementation by flapping wing MAVs. If they could be successfully replicated then flapping wing MAVs would have the potential to significantly outperform rotary wing MAVs in terms of manoeuvring and payload capacity, the latter being a critical aspect because of the miniature scale. This paper will analyse how pertinent aspects of insect flight can inspire optimal design of MAVs, and will describe the efforts being undertaken at the University of Bristol to meet this challenge.

2 BIOMIMETIC ANALYSIS OF INSECT FLIGHT

2.1 Biomimetic extraction

It has been stated that the principle interest in using biological inspiration for the purpose of designing a MAV is the unsteady aerodynamic mechanisms exploited by insects and certain avian species. The biomimetic designer therefore has to ascertain the optimum route to replicating these aerodynamic mechanisms. This can be done by considering the process of an insect wing beat in terms of four levels of abstraction. Ordered from initial action to final effect, these are the neuronal control signals that innervate muscle units, the flight apparatus connected to muscle, the wing kinematics that they produce and the aerodynamics that result. The 'depth' of biomimetic extraction is dictated by which of these levels are replicated. This section describes the latter three aspects of insect flight (flight apparatus, wing kinematics, and aerodynamic effect) so that the level of biomimicry most conducive to optimum MAV design can be determined. Although the neuronal impulses present in insects are analogous to engineering control signals, they are specific to muscle and do not translate to all actuation technologies so therefore will not be discussed.

2.2 Unsteady aerodynamic mechanisms

The very nature of unsteady aerodynamic mechanisms means it is difficult to predict their magnitude accurately (in terms of force production) for a specific wing stroke. An MAV is likely to share the inertia dominated laminar flow regime ($Re = 10^2$–10^4) of larger insects such as moths, rather than the viscosity dominated flow ($Re = 10^0$–10^2) inhabited by smaller insects such as flies [**3**]. Therefore, the unsteady aerodynamic mechanisms of interest are those thought to be used by larger insects, of which the main four are:

(a) leading edge vortex (LEV) and dynamic stall;
(b) wing rotation force;
(c) wake recapture;
(d) virtual mass.

The aerodynamic theory behind these mechanisms will not be given, as it has been previously reviewed in depth (Lehmann [**4**]; Sane [**5**]). Although it may not be feasible to design an MAV that can consistently reproduce all four mechanisms, utilizing the LEV and timing dependent wing rotation forces will be most critical to an MAV's flight performance. Studies involving dynamically scaled insect models have shown LEVs may produce up to two-thirds of the insect's weight in lift, while the wing rotation force contributed 35 per cent of the lift [**6**, **7**]. Significantly, this rotational force was dependent on the stroke reversal timing, indicating a clear correspondence between specific wing kinematics and aerodynamics. The relatively unpredictable nature of unsteady aerodynamic phenomena means that the primary route to replicating them is to use insect wing kinematics as a starting point before experimental or computational optimization techniques are considered.

2.3 Insect wing kinematics

The variation in unsteady aerodynamic phenomena utilized by different species of insect is due to factors such as distinct wing morphologies, local flow fields and most importantly (for design of MAVs) differing wing kinematics. Despite this variation, every wing stroke has two translatory stages (downstroke and upstroke) that are connected by two short rotational stages (supination and pronation), at which point the wing reverses direction. It is common to describe the motion of the wing through these stages using various *kinematic parameters*. Values of kinematic parameters vary greatly between different species of insect, so generalized values need to be defined.

The *wingtip trajectory* describes the path of the wing and is commonly described relative to a *stroke plane*, where the major component of translation is within the stroke plane. Although wingtip trajectories follow a three-dimensional spherical path, when considered as a two-dimensional side view they can all be described as being roughly elliptical in shape, with a downward curve. Examples of wingtip trajectories are shown in Fig. 1. The *stroke amplitude* is the maximum angle through which the wings move in the stroke plane and is usually around 120° [**8**]. The effective angle of attack is the wing's pitch relative to the wingtip trajectory and is usually at least 30° throughout the translatory stages of the wing stroke [**3**]. The timing

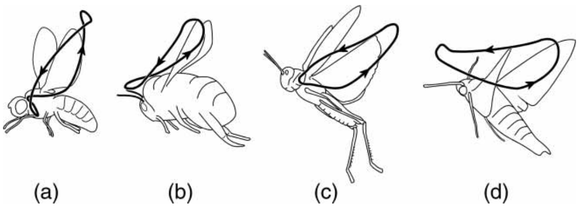

Fig. 1 Illustration of insect wing trajectories for (a) blowfly, *Calliphora erythrocephala*, (b) bumblebee, *Bombus hortorum*, (c) locust, *Locusta migratoria*, and (d) hawkmoth, *Manduca sexta*

of pronation/supination within the wing stroke is also important and is described as a ratio of the downstroke and upstroke (d/u), with values between 1 and 1.1 common [**2**]. Insects usually maintain a constant *wing beat frequency*, which varies inversely with body size for insects of a similar wing stroke. For larger insects this is between 20 and 40 Hz, but for small insects it may be up to 200 Hz [**9**]. The stroke plane angle and body angle usually vary concomitantly with speed, the former increasing and the latter decreasing.

In theory, matching the generalized kinematic parameter values listed above should result in the desired unsteady aerodynamic mechanisms being replicated. This, however, is not guaranteed; local flow fields will of course be significant and insects are known to alter their wing kinematics to suit specific aerodynamic demand [**10**]. Despite this, the generalized values do provide a starting point for an iterative optimization of MAV wing kinematics. Of more importance to designing an MAV capable of remaining airborne is the ability to adjust these parameters for flight stability or manoeuvring. An insect, like an aircraft or helicopter, has a total of six degrees of freedom (DOF). However, insects are only able to control a maximum of five of these DOF, since insects cannot accelerate laterally without rolling [**11**]. With more than five kinematic parameters, some of which can be adjusted symmetrically or asymmetrically across a pair of wings, this indicates that insects possess redundant control inputs. Rather than suggesting the insect flight control system is inefficient, these redundant control inputs will likely provide improved control for certain manoeuvres [**11**]. This is demonstrated in Table 1, which lists a summary of which kinematic parameters need to be altered for specific manoeuvres.

2.4 Flight apparatus and musculature

The flight apparatus and related musculature of insects is contained within the thoracic segments known as the pterothorax, with the exception of the wings which are connected via the axillary apparatus [**9**]. The pterothorax is composed of a complex combination of skeletal structures, axillary sclerites, resilin, and muscle units, meaning it is not feasible to reverse engineer it. Despite this there are still specific concepts that can be implemented in a flapping MAV design. The resilin, a highly elastic material, allows insects to store kinetic energy at the end of each upstroke and downstroke and release it to overcome the wing's inertia. The resilin also contributes to an important aspect of the pterothorax, the fact it is a mechanically resonant system. Insects maintain their wing beat frequency at the pterothorax's resonant frequency to further maximize muscle power output and efficiency.

The wing joint is complex in terms of the size, shape, and orientations of its elements, as well as their articulations. One common feature, however, is the use of indirect muscles to elevate the wings on the upstroke [**9**]. The muscles are described as indirect as they manipulate the top plate of the pterothorax, known as the notum, rather than the wing. Many orders of insect use the same arrangement to depress the wing with orthogonal indirect muscles causing the notum to arch upwards. Orders such as *Odonata*, *Ephemeroptera*, *Orthoptera*, and certain species of

Table 1 Kinematic parameter modulation required for performing manoeuvres (data from references [**3**], [**7**], [**11**], and [**12**])

Manoeuvre	Roll	Pitch	Yaw	Kinematic parameter	Wing balance
Forward acceleration		(X)		Stroke plane angle	Symmetric
		(X)		Stroke amplitude	Symmetric
		(X)		Wing beat frequency	Symmetric
Nose up/nose down		X		Stroke timing	Symmetric
Vertical acceleration				Stroke amplitude	Symmetric
Lateral acceleration	X			Stroke amplitude	Asymmetric
	X			Angle of attack	Asymmetric
Flat turn			X	Angle of attack	Asymmetric
			X	Stroke timing	Asymmetric
Banked turn	X		X	Stroke amplitude	Asymmetric
	X	X	X	Stroke plane angle	Asymmetric

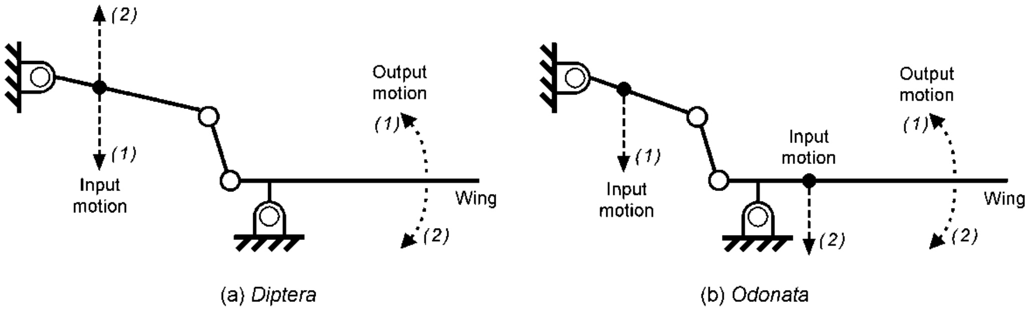

Fig. 2 Simplified two-dimensional rigid-body linkages representing the mechanics of the (a) *Dipteran* and (b) *Odonata* wing joint, where inputs (1) and (2) are alternated so that the wing elevates and depresses

Coleoptera use direct muscles instead. These attach directly to the wing, primarily through the basalar and subalar sclerites, so that the wing acts as a third-order lever. Therefore, all orders of insect use the lever principle, the simplest form of mechanical advantage, to maximize the muscle stroke output. Simplified mechanical representations of these lever arrangements for two insect orders that represent the two main types of pterothorax physiology are shown in Fig. 2. In this idealized rigid-body form a single wing can be said to be driven by a four-bar mechanism. It should be noted that the pterothoraxes of all insects also contain wing base muscles to subtly alter the wing stroke and wing angle of attack.

The final piece of flight apparatus that is due consideration for biomimetic extraction is the wing. Insect wings possess several features that maximize their lift-to-drag ratio while maintaining excellent mass efficiency. The arrangement and orientation of veins, which provide stiffness, ensure that insect wings have regions of favourable flexion lines within the compliant wing membrane [**13**]. The wings also have an inherently twisted and cambered shape that again increases the lift-to-drag ratio. Spanwise veins are often also arranged in peaks and troughs resulting in wing corrugation which improves stiffness. Also, the veins have a high mass efficiency, becoming elliptical in cross-section in areas where the loading is predominantly unidirectional.

2.5 Summary of biomimetic analysis

As outlined at the start of this section, a truly biomimetic approach to designing an insect-inspired MAV would involve replicating all aspects of insect flight. Since that would undoubtedly result in a non-optimal (and likely non-functional) solution, the following biomimetic guidelines are proposed.

1. The generation of unsteady aerodynamic mechanisms is critical, in particular LEVs (dependent on angle of attack and wing beat frequency) and rotation forces (dependent of angle of attack and stroke timing).
2. Replicating insect wing kinematics will provide a starting point for the above task.
3. Since wing kinematics vary greatly from species to species, generalized values of kinematic parameters for larger insects can be used.
4. For a flapping wing MAV to fly it must not just match insect wing kinematics, but know how to adjust them for manoeuvres (as listed in Table 1).
5. Mimicking certain aspects of insect morphology may be advantageous:
   (a) elastic storage and resonance increase efficiency and maximize power output;
   (b) mechanical advantage amplifies the primary muscles' output strain;
   (c) non-uniform vein shapes and orientations produce flexion lines and twisting to maximize the wing's lift-to-drag ratio.

3 CLASSIFICATION AND SELECTION OF FLAPPING MECHANISM

3.1 Assessment of actuators

The output requirements of an insect-inspired MAV flapping mechanism are defined by the wing kinematics described in section 2.3, while the input requirements are solely dependent on actuator selection. In most engineering design applications the mechanism can be designed for an arbitrary input stroke. MAVs' limited power supply and highly demanding mass and volume constraints, however, necessitate an integrated design process where actuator characteristics are explicitly addressed from an early stage [**12**]. Insect muscle, as all biological muscle, is characterized by a linear stroke with an extremely high strain output greater than any currently available linear actuator. Since any MAV flapping mechanism is required to be extremely compact, this is a significant issue.

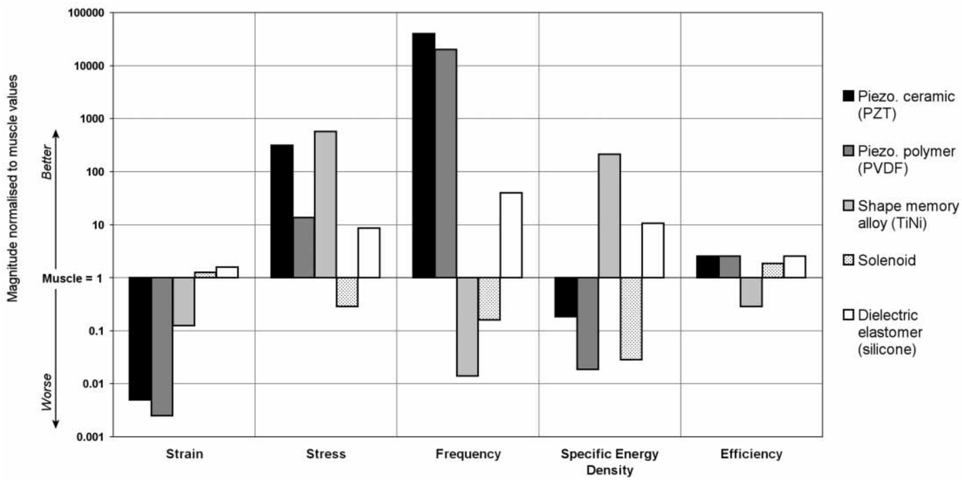

Fig. 3 Maximum performance of linear actuation technologies normalized to that of muscle (data from reference [**14**])

Figure 3 displays this disparity in strain output but also shows that man-made actuators generally outperform muscle for the other key performance characteristics for MAV actuation. In theory this suggests they may be viable when coupled with an amplification linkage but there are other issues to consider such as solenoid's low power density and shape memory alloy's low frequency range. Although piezoelectric ceramic can be constructed in a bimorph bender arrangement which greatly increases its strain output, it requires very large activation voltages. Novel actuation technologies such as electro-active polymers (e.g. piezoelectric polymers, dielectric elastomers) have shown the potential to produce a similar strain output as muscle, but many of these materials also require large activation voltages. It should be noted that the performance of any linear actuator may be improved by being activated at resonance, or within a resonant system. The alternative to linear actuation is the motor, which produces the equivalent of an unlimited output strain. At MAV scale there are piezoelectric motors and DC motors (brushless and brushed) available. Because of the added mass and volume of associated driver electronics that the first two options require, brushed DC motors can be considered to be the superior choice at this stage.

3.2 Mechanism classification

An insect-inspired MAV flapping mechanism has the principle purpose of driving the wings in a manner that maximizes lift and thrust through the production of unsteady aerodynamic phenomena, while allowing enough kinematical adjustability for flight stability and manoeuvring. It can be said that a secondary design specification of a linear input mechanism is to provide a high amplification ratio (to overcome limited actuator stroke output), while for a rotary input mechanism it is to convert rotary motion into controlled wing reciprocation.

An important aspect of these contrasting design specifications for linear and rotary input flapping mechanisms is the level of constraint they impose. A linear input mechanism can be *under-constrained* since, generally, a linear actuator can modulate the magnitude of its output stroke to allow proportional control. Rotary actuators cannot modulate their output stroke due to the fact they must continuously complete full revolutions, nor can they produce antagonistic outputs. This means a rotary input mechanism is more likely to have a constrained output i.e. the wing trajectory is fixed to a single path [**12**].

The consequences of a mechanism's level of constraint are summarized in Fig. 4. From Fig. 4, an

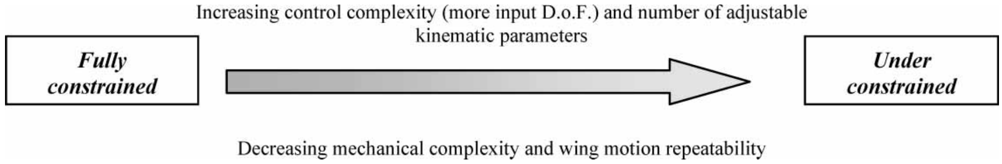

Fig. 4 Relationship between a mechanism's level of constraint and its performance and complexity [**12**]

under-constrained mechanism appears preferable as it offers optimum performance at the cost of increased control complexity, which does not necessarily add extra weight and volume. However, the relationship shown does not account for actuator performance (specifically limited strain output) and hence the mechanical realization of an under-constrained mechanism becomes less viable.

Since there are many mechanisms that may be considered for insect-inspired flapping, a figure of merit for ranking potential flapping mechanisms needed to be devised. The figure of merit developed uses a mechanism's level of constraint as a basis, with each mechanism rated in terms of mechanical complexity, control complexity, and performance. Mechanical complexity is based on the physical linkages (e.g. number of links and joints) and control complexity assesses the system's inputs and outputs (e.g. number of control parameters and actuators). For both types of characteristic, a higher total indicates higher complexity. It was assumed that the number of kinematic parameters a mechanism can adjust is a suitable measure of performance, as these directly govern flight stability and manoeuvrability.

A number of flapping mechanisms that have been previously published were assessed using this method of classification and the results are shown in Table 2. It should be noted that the majority of the mechanisms in Table 2 currently exist as precursor designs or experimental test-rigs and may therefore have intentionally limited capabilities. Table 2 also includes a two-winged *Dipteran* insect for comparison. Its control complexity was calculated by summing the known flight muscles and corresponding motor neurones as described in biological literature [**15**]. The mechanical complexity was more difficult to quantify accurately, but using the description of a generic wing joint morphology by Snodgrass [**16**] an estimate was achieved. It is assumed the *Dipteran* insect has four controllable body DOF, larger insects and dragonflies are believed to have five [**11**].

The main conclusion from Table 2 is that, as expected, almost all rotary-input mechanisms produce constrained outputs that inhibit modulation of wing kinematics. In addition, it was also found that almost no mechanism could incorporate full three DOF wing control by itself. This makes it necessary to have one mechanism to produce the desired wing trajectory (one or two DOF) and another for wing pitching (one DOF), which adds extra links and actuators and hence mass and volume. Constrained linkages with adjustable DOF, commonly referred to as metamorphic mechanisms, do not constitute a viable solution as switching between phases during flight would be impractical because of the high wing beat frequencies. With respect to these limitations, a flapping mechanism based on a PCR arrangement was conceived and selected for development. This mechanism has a rotary-input, combined control of wing flapping and pitching and is only partially constrained meaning certain kinematic parameters can be adjusted.

3.3 PCR mechanism

The PCR mechanism consists of a pair of PCR linkages per wing, where the output links (known as rockers) within each linkage pair are coupled using the articulation shown in Fig. 5. Since one rocker is attached to the wing's leading edge and the other to its trailing edge, the wing's angle of attack can be controlled by introducing a phase lag between the two linkages. This integrated method of controlling wing pitching through the anterior edges of the wing is similar to that employed by insects and allows for faster angular acceleration of the wing than a separate pitching mechanism. By adjusting the size of the phase lag between the two inputs (cranks) the midstroke angle of attack or rotation timing at stroke reversal can be altered. This allows for control over the kinematic parameters that have the most critical influence on the two most important unsteady aerodynamic mechanisms (as described in section 2.2).

In terms of complexity, the PCR mechanism has a slightly higher control complexity than the other rotary mechanisms and an approximately average mechanical complexity. However, the PCR allows for superior performance over the other rotary-input mechanisms as it is not fully constrained because of the free coupling between the parallel rockers. This allows asymmetric control of the wing angle of attack, which in conjunction with adjustable wing beat frequency (motor speed control) gives a total of four controllable body DOF based on the insect manoeuvre information in Table 1. For the PCR mechanism to offer full functionality, an actuator is required to control the phase lag of each pair of parallel cranks, with a third actuator providing the primary rotary drive for flapping.

The most interesting point of comparison between the man-made and insect flapping mechanisms is their relative ratios of complexity to performance. This is best viewed by extending the mechanism assessments in Table 2 into a bar chart, so that a unique system profile can be created for each mechanism. For clarity only the PCR mechanism and *Dipteran* insect have been included in Fig. 6. This method of

Table 2 Complexity and performance classification of two-winged MAV flapping mechanisms

Mechanism	Five-bar coupler with four-bar [17]	Four-bar coupler and Geneva wheel [18]	Scotch yoke [19]	Double scotch yoke and Geneva wheel [20]	Non-planar crank-rocker [21]	Parallel crank-rockers	Parallel four-bars [22]	*Dipteran* (two-winged insect)
Simplified kinematic diagram	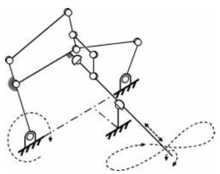	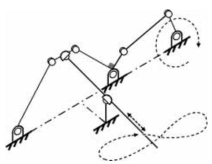	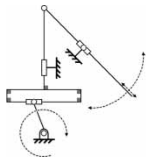	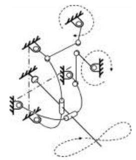	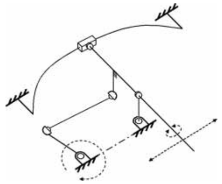	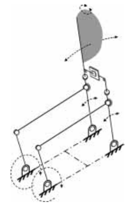	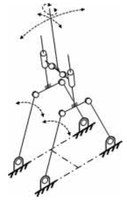	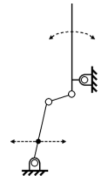
Complexity								
Control								
Input type	Rotary	Rotary	Rotary	Rotary	Rotary	Rotary	Linear	Linear
Control inputs	1	1	1	1	1	3	8	12
Acutators	1	1	1	1	1	3	8	50
Mechanical								
Sliding joints	2	3	6	5	2	2	0	0
Revolute and spherical joints	17	13	6	22	10	18	38	38
Non-grounded links	12	9	6	16	10	12	18	20
Performance								
Key kinematic parameters								
Wing trajectory	Fixed two DOF	Fixed two DOF	Fixed one DOF	Fixed two DOF	Fixed one DOF	Fixed one DOF	Adjustable one DOF	Adjustable two DOF
Angle of attack, α	Fixed	Fixed	Fixed	Fixed	Fixed	Adjustable	Adjustable	Adjustable
Stroke amplitude, Φ	Fixed	Fixed	Fixed	Fixed	Fixed	Fixed	Adjustable	Adjustable
Timing, d/u	Fixed	Fixed	Fixed	Fixed	Fixed	Fixed	Adjustable	Adjustable
Controllable body DOF	1	1	1	1	1	4	4	4

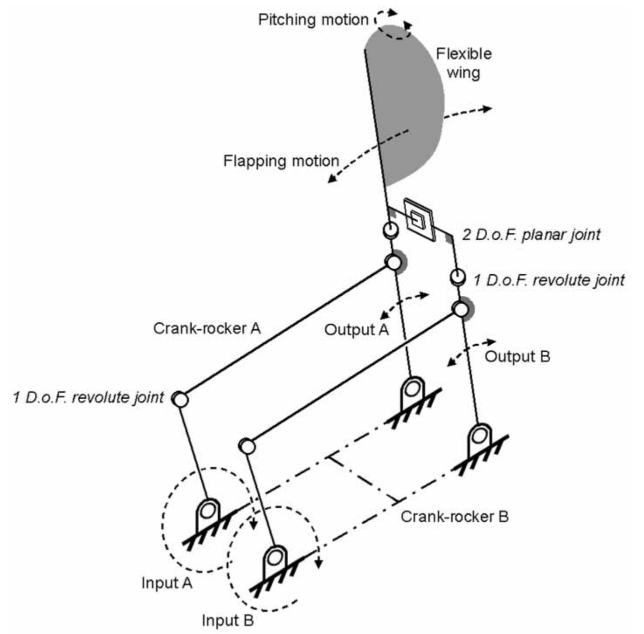

Fig. 5 Kinematic sketch of the parallel crank-rocker mechanism. The flapping motion is the product of output motions A and B, while the pitching motion results when there is a phase lag between output A and B (and hence inputs A and B)

system profiling clearly shows the increased complexity of the insect is not matched, in theory, by increased performance (in terms of controllable body DOF). What can, therefore, be concluded is that insects utilize control redundancy, as described in section 2.3 and may be expected to have increased manoeuvring ability.

4 PROTOTYPE DEVELOPMENT AND TESTING

4.1 Design and manufacture

To validate the concept of the PCR flapping mechanism a prototype has been developed. As well as providing a proof of concept, the PCR prototype also acts as an experimental test-rig for wing kinematics optimization. The ultimate aim of this optimization is to gain a clearer understanding of the effect wing kinematics have on unsteady aerodynamics and, therefore, lift production. A kinematic analysis of possible link lengths suggested that the ratio 1:3.8:1.3:4 (crank:coupler:rocker:ground) provides the closest match to the generalized insect wing kinematics described in section 2.3, with a stroke amplitude of 102° and stroke timing (d/u ratio) of one. A larger stroke amplitude and hence increased aerodynamic power is achievable with alternative link ratios, but these were rejected on the basis that they cause the transmission angle (the angle between coupler and rocker) to exceed the desirable range of 40°–140°.

As previously described, a fully-functional system would require an actuator to control the phase lag of each pair of parallel cranks, with a third actuator providing the primary rotary drive. However, for the purposes of an experimental test-rig it was decided that the crank phase lag should be adjusted manually (i.e. when the primary drive is stopped) so that the prototype only requires a single motor.

Full dynamic analysis of the PCR prototype design was completed prior to manufacture using a combined rigid-body and electro-mechanical model in the SIMULINK® SimMechanics environment. Based

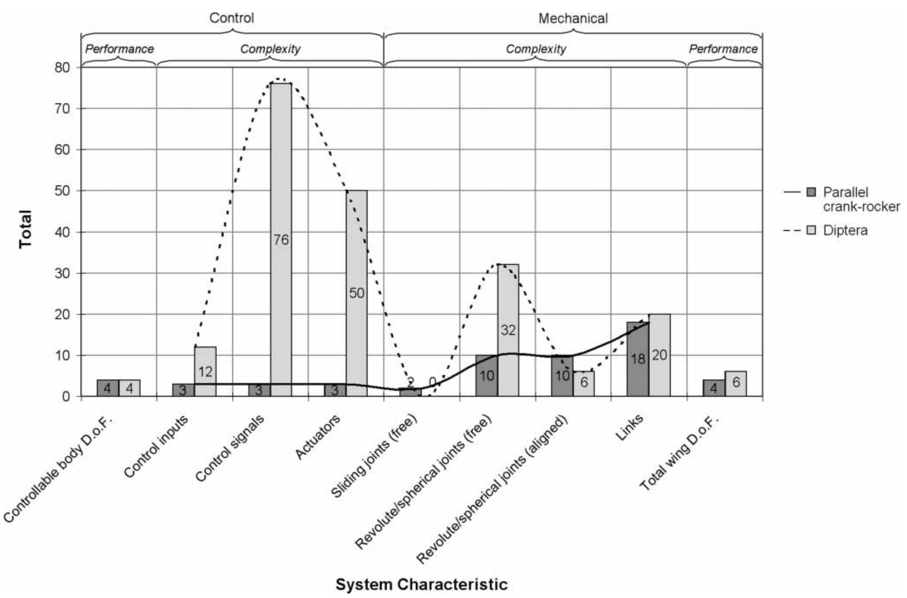

Fig. 6 The system profiles of the PCR mechanism and a *Dipteran* insect, with system complexity and performance metrics grouped into control and mechanical characteristics

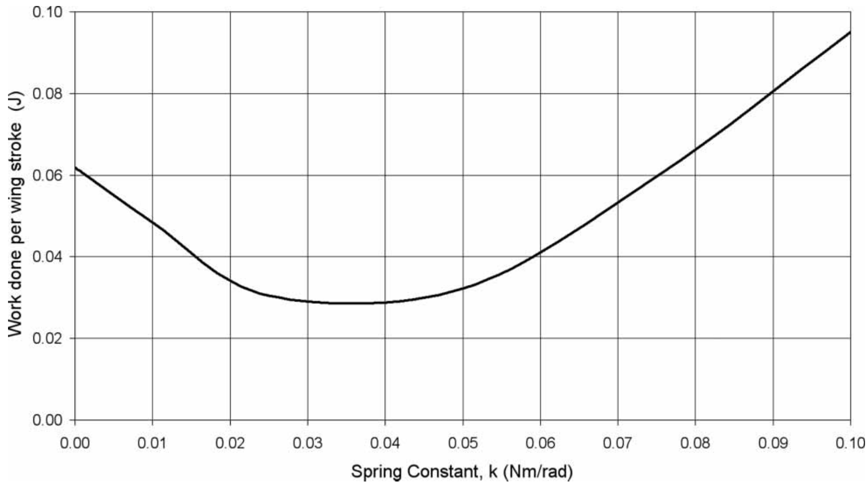

Fig. 7 Simulated effect of elastic storage on the work done per wing beat, showing that the optimum spring constant is around 0.03–0.04 Nm/rad for a wing beat frequency of 50 Hz and wing mass of 1 g

on the results of this model the link geometry was optimized for minimum dynamic forces and a Maxon RE10 brushed motor (7 g mass) with a 2.9:1 gear ratio was selected. The results from the model also proved that the use of elastic storage, extensively employed by insects, is extremely beneficial and can reduce the work done per wing stroke by up to 50 per cent as shown in Fig. 7.

For the manufacture of the PCR prototype, dynamic scaling was eschewed in favour of full-scale 75 mm long wings with approximately 2:1 scale linkages and base components. The purpose of manufacturing at near-MAV scale was to test in-house microfabrication capabilities. Excluding the wings, the complete assembly has major dimensions of 25 × 29 × 62.75 mm. The finished prototype mechanism is shown in Fig. 8, with wings constructed from carbon rods and Mylar®. The majority of the parts from the main assembly are manufactured from aluminium, so despite being designed as an experimental test-rig the total weight is just 46 g, excluding power supply.

4.2 Prototype testing

The initial stage of testing carried out on the prototype involved verifying that the wing kinematics matched predicted values. A Photron DVR high-speed camera was used to film the prototype in operation. The 500 frames per second footage from this camera allowed the wing beat frequency, flapping angle and angle of attack to be measured manually. Figure 9 shows plots of the measured flapping angle and angle of attack over a wing beat compared with predicted values. The deviation of the measured flapping angle values from the predicted curve on the downstroke is likely to be due to motor speed fluctuations (as discussed later in this section). Even with the high-speed camera, there was still difficulty in measuring the angle of attack accurately due to the wing twisting, so human error can be attributed to the deviation in the data. Despite this, there is a reasonably close correlation between the measured and predicted values. The testing was undertaken with the crank phase lag at 20°, which gives

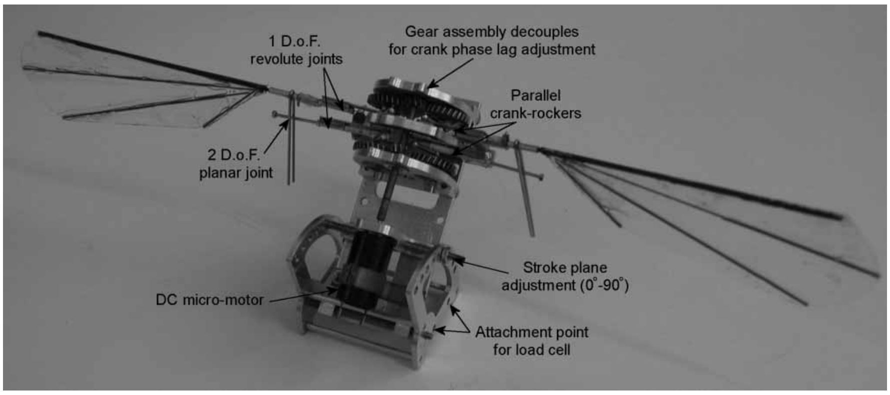

Fig. 8 The finished PCR test-rig with key features annotated

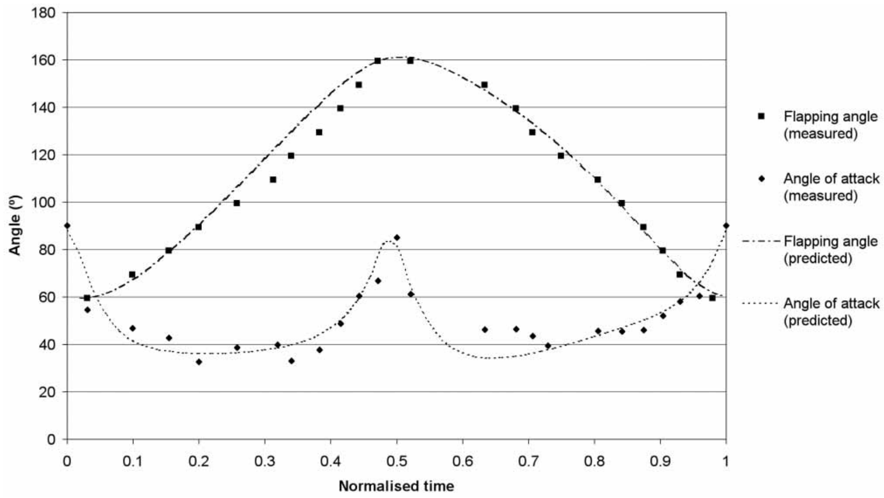

Fig. 9 Plots of the measured and predicted flapping angle and angle of attack over a wing beat (downstroke: $t' = 0$–0.5; upstroke $t' = 0.5$–1) with a crank phase lag of 20°. The flapping angle is taken from horizontal while the angle of attack is measured with respect to the wing trajectory

a midstroke angle of attack of approximately 35° as shown in Fig. 9. Increasing the phase lag would have decreased the angle of attack and vice versa.

One of the most important performance characteristics for any MAV prototype is the wing beat frequency. The SIMULINK® SimMechanics dynamic model predicted a wing beat frequency of around 15 Hz. However, the measured wing beat frequency was found to be only 5.52 Hz, with the DC motor running at its rated maximum supply voltage of 6 V. The predominant cause of this significant reduction is greater than the expected friction between the gears, most likely due to shaft misalignment during manufacture. It was also observed from the high-speed footage that at stroke reversal the mechanism slowed to a near standstill due the wing inertia resisting the change in direction. This effect is shown in Fig. 10, which shows how the motor speed fluctuates throughout the wing beat. Note how the motor has to accelerate the wing, gears, and links from a very low speed after every stroke reversal.

The biomimetic solution of elastic storage was implemented to resolve the problem of speed fluctuations, with miniature springs added to each wing. Due to a restricted selection of off-the-shelf miniature springs, three different pairs of springs were tested. The results indicate that these had a limited effect on mechanism energetics. The best-performing pair of springs increased the wing beat frequency to 6.15 Hz and reduced the work done per wing beat from 21.64 to 20.51 mJ. Since there is no indication of how close the selected spring constant of 15.9 N/m is to

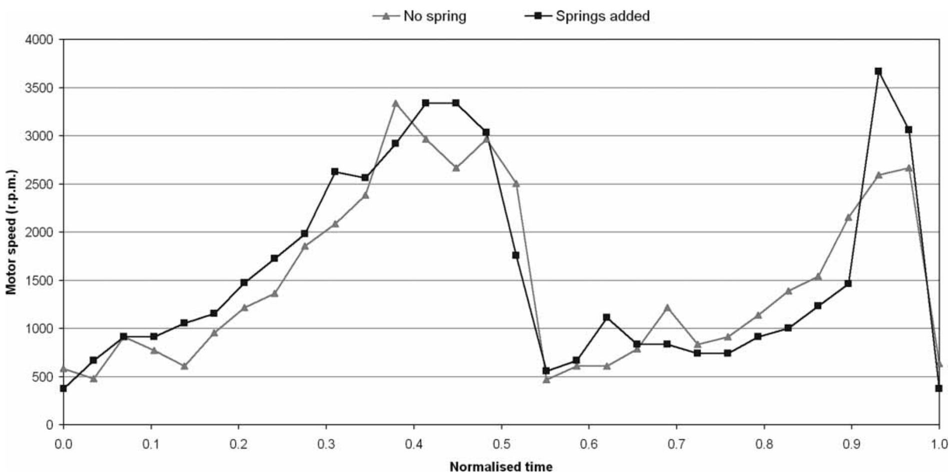

Fig. 10 Plots of motor speed over a wing beat for the mechanism with and without elastic storage (upstroke: $t' = 0$–0.5; downstroke: $t' = 0.5$–1)

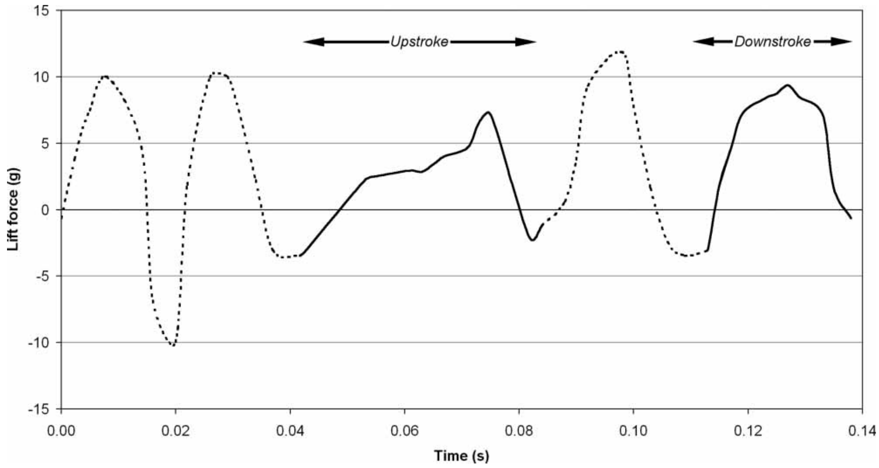

Fig. 11 Plot of lift force over a complete wing stroke cycle with a wing beat frequency of 7.15 Hz. The solid line shows the lift produced during the downstroke and upstroke whereas the dashed line represents the oscillating inertial reaction force that occurs at wing reversal

the optimum value, it is difficult to predict what the maximum achievable wing beat frequency is. However, the results from the SimMechanics simulation (as shown in Fig. 7) suggest that if the optimum spring constant was applied, the motor speed fluctuations would be smoothed out and wing beat frequency would correspondingly increase significantly.

The aerodynamic performance of the prototype (without elastic storage) was also tested by measuring the lift force produced in a hovering orientation. Lift was measured using a single-axis load cell with the sensing direction aligned perpendicularly to the horizontal stroke plane. The data obtained from this experimental set-up showed that an inertial reaction force was dominant at wing reversal. Inspection of the high-speed camera footage confirmed that the wings oscillate out of the stroke plane at this point in the wing stroke. This is likely to be caused by a combination of the relatively poor transmission angle at that point in flapping cycle and the high inertial force resisting the wing's reversal. The exact magnitude of these inertial forces was isolated using dummy wings with identical inertial properties but no wing membrane (and hence minimal aerodynamic forces). In addition, the acquired data was processed using a fourth-order Butterworth low-pass filter to eliminate high frequency noise. The lift produced over a single wing beat by the prototype running at 7.15 Hz is shown in Fig. 11 (the motor was run above the rated voltage with a 7-V DC supply to achieve the increased wing beat frequency). The mean lift for the total wing stroke shown in Fig. 11 is 3.35 g, while it is 2.40 g and 4.87 g for the upstroke and downstroke phases, respectively. These values of mean lift indicate that the current prototype needs to be driven at a higher wing beat frequency before flight can be considered, since the fully-functional MAV will be likely to have a mass of at least 10 g. This result strongly favours the implementation of the optimized elastic storage discussed previously in future prototype development.

5 CONCLUSIONS

In the current paper, a novel mechanism for replicating insect wing kinematics has been presented. The challenges posed by trying to replicate insect flight were discussed, with generalized kinematic parameters and biomimetic design guidelines proposed as a result. As well as identifying absolute values of kinematic parameters, a summary of how insects manipulate these parameters to enact aerobatic manoeuvres has been compiled. These provided a specification upon which an actuated flapping mechanism can be designed to meet. Due to the variety of potential mechanisms suitable for this task, an original method of classifying and ranking flapping mechanisms was conceived. This method takes account of a mechanism's mechanical and control complexity in relation to its performance. A novel mechanism called the PCR was compared with previously published flapping mechanisms using this classification method. It was found that the PCR mechanism has a similar level of complexity as other mechanisms, but improved performance attributed to its integrated partially-constrained design.

The PCR concept was developed into a functional test-rig prototype with 75 mm long wings. Initial testing was carried out on the PCR mechanism, which involved verifying that the wing kinematics matched the desired values. Both the flapping angle and adjustable angle of attack closely matched predicted values, but the wing beat frequency of 5.5 Hz was significantly lower than a simulated model. This reduction in frequency is believed to be caused by a combination of increased friction because of misaligned gears and the lack of elastic storage at stroke reversal. An attempted solution to the latter problem had a limited effect, with a slight increase in the wing beat frequency to 6.15 Hz. However, this was with a limited selection of non-optimized springs so it is believed that an improved spring constant would have a much more pronounced effect on increasing the wing beat frequency. A single-axis load cell was used to measure the lift produced by the prototype in a hovering configuration. The mean lift over a single wing beat was found to be 3.35 g at a flapping frequency of 7.15 Hz.

ACKNOWLEDGEMENTS

This work is supported by the UK Engineering and Physical Sciences Research Council (EPSRC) through grant number EP/C535286/1. The authors would also like to thank the EPSRC Engineering Instrument Pool for loaning the Photron DVR camera.

REFERENCES

1 **McMichael, J. M.** and **Francis, M. S.** Micro air vehicles – toward a new dimension in flight, 1997. DARPA document, available from http://www.fas.org/irp/program/collect/docs/mav_auvsi.htm.

2 **Ellington, C. P.** The aerodynamics of hovering insect flight. III. Kinematics. *Philos. Trans. R. Soc. Lond. B, Biol.*, 1984, **305**, 41–78.

3 **Ellington, C. P.** The novel aerodynamics of insect flight: applications to micro-air vehicles. *J. Expl. Biol.*, 1999, **202**, 3439–3448.

4 **Lehmann, F. O.** The mechanisms of lift enhancement in insect flight. *Naturwissenschaften*, 2004, **91**(3), 101–122.

5 **Sane, S. P.** The aerodynamics of insect flight. *J. Expl. Biol.*, 2003, **206**, 4191–4208.

6 **Van den Berg, C.** and **Ellington, C. P.** The three-dimensional leading-edge vortex of a 'hovering' model hawkmoth. *Philos. Trans. R. Soc. Lond. B, Biol.*, 1997, **352**, 329–340.

7 **Dickinson, M. H., Lehmann, F. O.,** and **Sane, S. P.** Wing rotation and the aerodynamic basis of insect flight. *Science*, 1999, **284**, 1954–1960.

8 **Brodsky, A. K.** *The evolution of insect flight*, 1994 (Oxford University Press, Oxford).

9 **Dudley, R.** *The biomechanics of insect flight: form, function, evolution*, 2000 (Princeton University Press, Princeton, NJ).

10 **Willmott, A. P.** and **Ellington, C. P.** The mechanics of flight in the hawkmoth, *Manduca sexta*. I. Kinematics of hovering and forward flight. *J. Expl. Biol.*, 1997, **200**, 2705–2722.

11 **Taylor, G. K.** Mechanics and aerodynamics of insect flight control. *Biol. Rev. Camb. Philos. Soc.*, 2001, **76**(4), 449–471.

12 **Conn, A. T., Burgess, S. C.,** and **Hyde, R. H.** Development of a novel flapping mechanism with adjustable wing kinematics for micro air vehicles. In *Design and nature III* (Ed. C. A. Brebbia), 2006, pp. 277–286 (WIT Press, Southampton).

13 **Wootton, R. J.** Functional morphology of insect wings. *Annu. Rev. Entomol.*, 1992, **37**, 113–140.

14 **Bar-Cohen, Y.** *Electroactive polymer (EAP) actuators as artificial muscles–reality, potential and challenges*, 2nd edition, 2004 (SPIE Press, Bellingham, WA).

15 **Chapman, R. F.** *The insects: structure and function*, 1998 (Cambridge University Press, Cambridge, UK).

16 **Snodgrass, R. E.** *Principles of insect morphology*, 1935 (McGraw-Hill, New York, USA).

17 **Banala, S.** and **Agrawal, S. K.** Design and optimization of a mechanism for out-of-plane insect winglike motion with twist. *Trans. ASME, J. Mech. Des.*, 2005, **127**, 841–844.

18 **Żbikowski, R., Galiński, C.,** and **Pedersen, C. B.** A four-bar linkage mechanism for insect-like flapping wings in hover: concept and an outline of its realisation. *Trans. ASME, J. Mech. Des.*, 2005, **127**, 817–824.

19 **Tarascio, M. J., Ramasamy, M., Chopra, I.,** and **Leishman, J. G.** Flow visualization of micro air vehicle scaled insect-based flapping wings. *J. Aircr.*, 2005, **42**(2), 385–390.

20 **Galiński, C.** and **Żbikowski, R.** Insect-like flapping wing mechanism based on a double spherical Scotch yoke. *J. R. Soc. Interface*, 2005, **2**(3), 223–235.

21 **Burgess, S. C., Alemzadeh, K.,** and **Zhang, L.** The development of a miniature mechanism for producing insect wing motion. In *Design and nature II* (Eds M. W. Collins and C. A. Brebbia), 2004, pp. 237–244 (WIT Press, Southampton).

22 **Avadhanula, S., Wood, R. J., Steltz, E., Yan, J.,** and **Fearing, R. S.** Lift force improvements for the micromechanical flying insect. IEEE International Conference on Intelligent Robots and Systems, October 2003, pp. 1350–1356 (Las Vegas, Nevada).